# Photo-induced liquid crystal alignment on polyimide containing fluorinated groups

Shi-Joon Sung; Jong-Woo Lee; Hee-Tak Kim; Jung-Ki Park

## PLEASE SCROLL DOWN FOR ARTICLE

# Photo-induced liquid crystal alignment on polyimide containing fluorinated groups

SHI-JOON SUNG, JONG-WOO LEE, HEE-TAK KIM† and JUNG-KI PARK*

Department of Chemical Engineering,
Korea Advanced Institute of Science and Technology, 373-1 Yusung-gu,
Kusung-dong, Daejon 305-701, Korea
†New Energy Storage Systems, Wonchon-dong, Paldal-gu, Suwon 442-749, Korea

Polyimides were prepared from pyromellitic dianhydride, 4,4′-bis[2-(4-aminophenyl)hexa-fluoroprop-2-yl]diphenyl ether and 4,4′-diamodiphenyl ether (PMDA-BDAF-ODA) and used for liquid crystal alignment using linearly polarized UV exposure. The alignment properties of a LC on the polyimide films were found to depend on the fluorine content in the PMDA-BDAF-ODA alignment layer and on the UV exposure time. Pretilt angles were obtained in the range 0° to 90° dependent upon the fluorine content in the polyimide film and the UV exposure time. These effects seem to be closely related to the surface energy of the photo-alignment layer.

## 1. Introduction

The surface alignment of liquid crystal (LC) molecules is of great importance in the fabrication of liquid crystal displays (LCDs), and much work on this topic has been carried out. Nowadays, to align LC molecules, the process of rubbing the surface of a polyimide film is usually adopted in manufacturing LCDs. However, this process has problems such as generation of static charge, dust, or scratches caused by rubbing. Therefore the establishment of a rubbing-free method is an important target making it possible to overcome the problems in the rubbing process. LC alignment using ultraviolet (UV) exposure is a promising candidate for use as a non-rubbing method [1], but generation of a pretilt angle using this technique is known to be difficult. Control of the pretilt angle of LC alignment is very important in order to achieve display uniformity in LCDs, the pretilt angle preventing creation of disclinations. The properties of the aligning surface are very important in understanding the mechanism of the generation of pretilt angle. It has been reported that the high pretilt angle generated in 4-*n*-pentyl-4′-cyanobiphenyl (5CB) on rubbed polyimide surfaces containing trifluoromethyl moieties is due to the fluorine atoms in the surface of alignment layer [2]. Some studies have been carried out on the relationship between the surface energy of the rubbed alignment layer and the pretilt angle generated in the liquid crystal [3]; there have been no such studies on non-rubbed alignment.

In this paper, we present a study of photo-induced LC alignment on polyimide substrates containing trifluoromethyl moieties. Special attention is paid to the dependence of pretilt angle on the fluorine content in the alignment layer and the UV exposure time. The effects of the surface energy and morphology of the alignment layer on the pretilt angle of the liquid crystal were also investigated.

## 2. Experimental

### 2.1. *Synthesis of polyimides*

The PMDA-BDAF-ODA polyamic acid precursor of the PMDA-BDAF-ODA polyimide was synthesized by adding an equimolar amount of pyromellitic dianhydride to an *N*-methyl-2-pyrrolidone (NMP) solution of a mixture of 4,4′-bis[2-(4-aminophenyl)hexafluoroprop-2-yl]-diphenyl ether (BDAF) and 4,4′-diaminodiphenyl ether (ODA) at room temperature under a nitrogen atmosphere. The amount of DBAF used in the feedstock was varied between 10 and 50 mol% (see table 1). The solution was stirred for 10 h at room temperature, and then poured into an excess of methanol. The precipitate was filtered off and dried *in vacuo* at room temperature.

Table 1. BDAF content (mol%) in the synthesized PMDA-BDAF-ODA polyimide.

| Sample | F07 | F17 | F21 | F43 |
|---|---|---|---|---|
| Feed | 10 | 20 | 30 | 50 |
| Polyimide | 6.6 | 17.4 | 21.2 | 43.0 |

*Author for correspondence; e-mail: pjk@mail.kaist.ac.kr

### 2.2. *Characterization of polyimides*

The structures of the polyimides were characterized using proton nuclear magnetic resonance spectroscopy (Bruker-AMX-500 NMR spectrometer, Bruker). For the NMR experiments, we prepared the polymer solutions (0.1 g cm$^{-3}$) using dimethylsulphoxide-d$_6$. Tetramethylsilane was used as an internal reference for peak assignments.

### 2.3. *Preparation of alignment layers*

A 2 wt% NMP solution of PMDA-BDAF-ODA polyamic acid was spin-coated onto the glass substrate at 1800 rpm and the cast film was prebaked at 60°C for 30 min. Thermal imidization of the cast film was then conducted at 180°C for 1 h. After the thermal imidization of the polyamic acid alignment layer, the photo-reaction of the polyimide was carried out by irradiating with polarized UV light to give the alignment layer. Polarized UV light for irradiation of the polymer thin films was obtained by passing light from a 300 W high pressure mercury arc (Oriel) through a UV linear dichroic polarizer (27320, Oriel) and a UV filter (51650, Oriel). The intensity of the irradiating UV light measured using a UV detector (UIT-150, Ushio) was 5 mW cm$^{-2}$. To provide a certain pretilt angle of the nematic liquid crystal, the alignment layers were first exposed to polarized UV perpendicular to the alignment layer and then to unpolarized UV at an oblique angle to the alignment layer.

### 2.4. *Surface energy measurement*

The surface energy of the PMDA-BDAF-ODA polyimide alignment layer in terms of the varying BDAF content in the PMDA-BDAF-ODA polyimide, was calculated from water and ethylene glycol contact angles on the alignment layer. The polar, dispersion, and total surface energies were calculated using the Girifalco–Good–Fowkers–Young equation [4].

### 2.5. *Scanning probe microscopy*

Atomic force microscopy was used to obtain topographical information about the dried substrate surface. The analysis was conducted, in the tapping mode, with a commercial instrument (Nanoscope IIIa, Digital Instrument Co.) equipped with a TESP (silicon crystal) tip.

### 2.6. *X-ray photo-electron spectroscopy*

X-ray photo-electron spectroscopy (XPS) analysis for the blend layers was carried out using a monochromatic micro-spot X-ray beam originating from a MgK$_\alpha$ source (1253.6 eV photons) with a spot diameter of $\cong 600$ μm stemming from a Surface Analysis System SPECS LHS10 spectrometer. The X-ray source was run at a reduced power of 120 W (12 kV and 10 mA). Throughout the measurement, the pressure in the analysis chamber was maintained at 10$^{-8}$ mbar or lower. To compensate for any surface charging effect, all binding energies (BE) were calibrated with reference to the neutral carbon C1s line taken at 284.6 eV.

### 2.7. *Preparation of LC cells*

A homogeneously aligned LC cell was constructed by sandwiching the nematic LC (E7) between a pair of glass substrates covered with a thin film of the polyimide. The thickness of the LC layer was adjusted by adhesive tapes of 50 μm thickness. E7 liquid crystal in the isotropic phase was introduced into the cell by capillary action.

### 2.8. *Pretilt angle measurement*

The pretilt angle of the nematic LC was measured by the crystal rotation method as described elsewhere [5]. The pretilt angles were determined from the plot of the transmittance as a function of the incidence angle of the He-Ne laser beam used as a probing light and passing through the cell set between two crossed polarizers.

### 3. Results and discussion

#### 3.1. *Preparation of PMDA-BDAF-ODA polyimide copolymers*

The syntheses of the PMDA-BDAF-ODA polyimide copolymers were carried out as indicated in figure 1. The polyimides derived from PMDA, ODA, and BDAF were obtained as white powders by precipitating their solutions with methanol. For brevity, the PMDA-BDAF-ODA polyimide copolymer will be designated in this paper as F*n*, where *n* indicates the mol% of the monomeric unit of BDAF in the polyimide.

The $^1$H NMR spectra of PMDA-ODA, PMDA-BDAF, and PMDA-BDAF-ODA are shown in figure 2. For the PMDA-ODA homopolymer, the proton peaks in the benzene ring of the diamine unit are designated a and b, and for the PMDA-BDAF homopolymer, the proton peaks in the benzene ring of the diamine unit are designated 1, 2, 3, and 4. From the relative proton peak areas corresponding to PMDA-ODA and PMDA-BDAF diamine units, it was possible to calculate the relative content of BDAF diamine unit in the PMDA-BDAF-ODA polyimide (table 1).

#### 3.2. *Liquid crystal alignment on the PMDA-BDAF-ODA polyimide alignment layer*

In order to examine the photo-induced liquid crystal alignment on the thin layer of PMDA-BDAF-ODA polyimide, parallel aligned LC cells were prepared. The irradiation energy applied to the alignment layer was
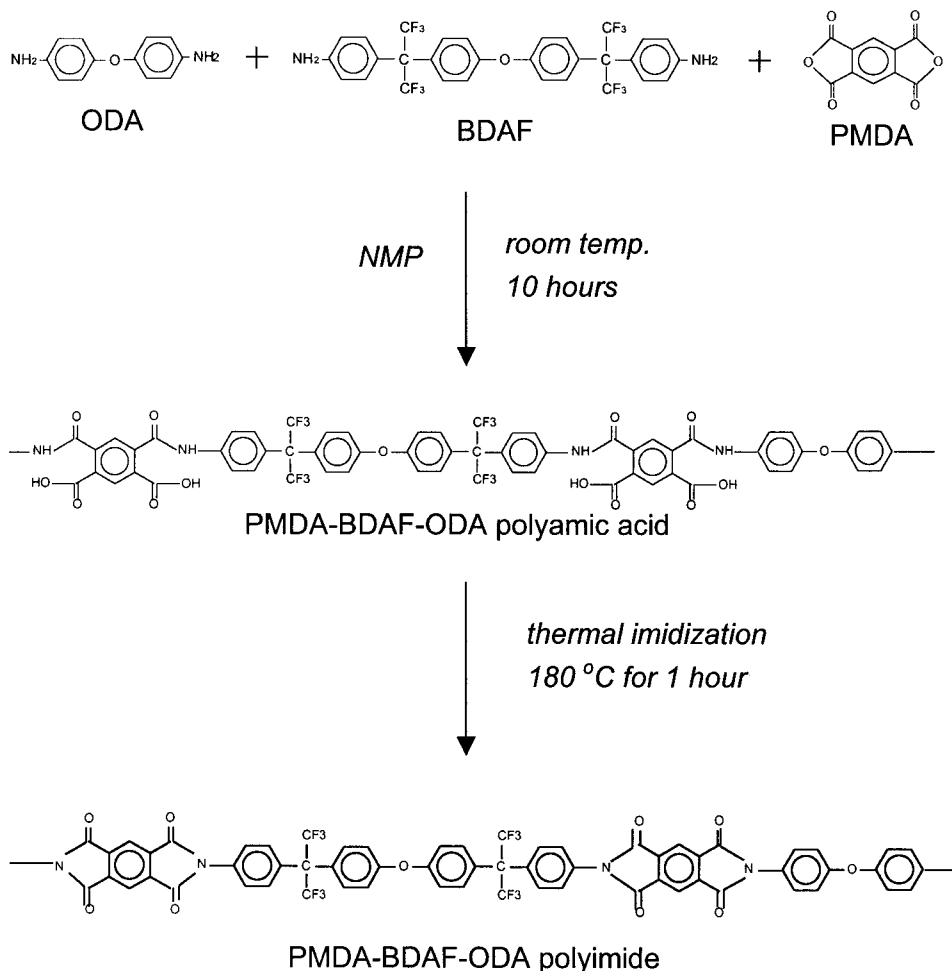
Figure 1.   Synthetic scheme for the PMDA-BDAF-ODA polyimide.

$9\,\mathrm{J\,cm^{-2}}$. Figure 3 displays the polarized microscopic images of the LC cells prepared with the alignment layers based on the PMDA-BDAF-ODA polyimide. The dark and light images repeatedly appear on rotating the LC cell between crossed polarizers and this behaviour is characteristic of homogeneous alignment. The high contrast between the dark and light images indicates that the liquid crystal alignments are quite uniform. All of the polyimide alignment layers with various BDAF contents show this good homogeneous liquid crystal alignment. From this result, it is reasonable to conclude that the PMDA-BDAF-ODA polyimide can be used for photo-induced LC alignment layers.

### 3.3. *Effect of BDAF content in the copolymer on pretilt angle*

In order to generate the LC pretilt angle required for avoiding reverse tilt disclinations, we utilized a modified double exposure method. It has been reported that the double exposure method, which involves a first exposure of linearly polarized UV and a second exposure

of p-polarized UV at oblique incidence, is effective in generating pretilt angles [6]. In this case, the polarization direction for the first exposure and that of the p-polarized UV of the second exposure are perpendicular; this is due to the direction of the LC alignment on the polyimide induced by the polarized UV irradiation being perpendicular to the polarization direction. In our work, the double exposure method was modified such that unpolarized UV was used in the second exposure instead of p-polarized UV. Since the electric vector of the p-polarized UV for the second exposure and that of the linearly polarized UV for the first exposure are perpendicular to each other, the second exposure can often reduce the degree of unidirectional LC alignment. Therefore, unpolarized UV, in which the s-polarized component is parallel to the polarization direction of the first exposure, was employed as the UV light for the second exposure in our experiment. This preserves the unidirectional alignment induced during the first exposure, and the p-polarized component provides a certain pretilt angle.
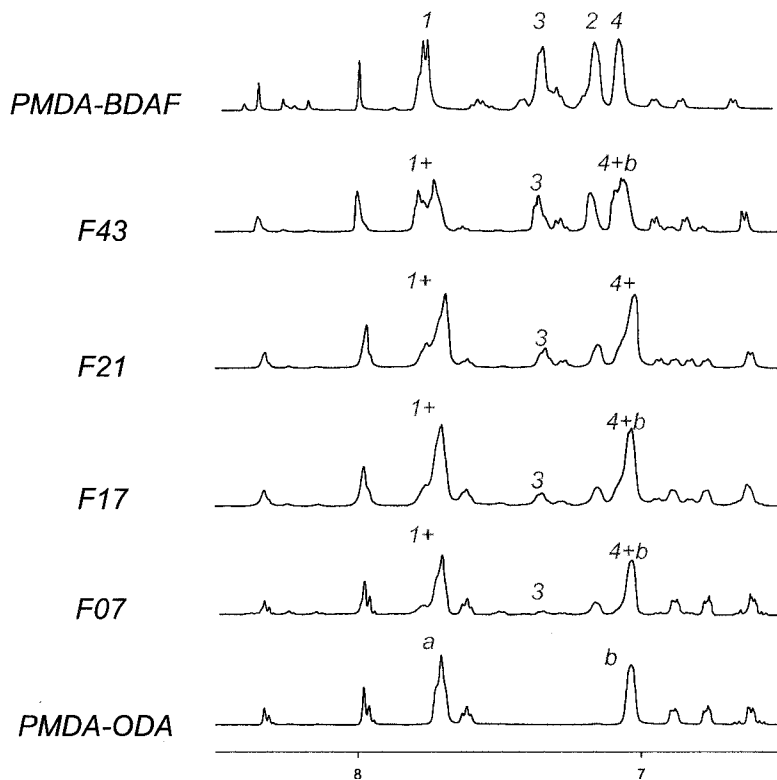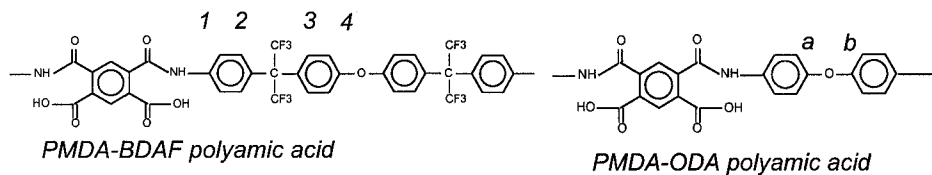
PMDA-BDAF polyamic acid

PMDA-ODA polyamic acid



Figure 2.   ¹H  NMR  spectra  for
polyimides with various BDAF
contents.

By using the modified double exposure method, we succeeded in producing higher pretilt angles of 4° for the F21 polyimide alignment layer. Figure 4 shows a plot of the pretilt angle of E7 as a function of BDAF content in the polyimide alignment layer.

Polarized UV of $9\,\mathrm{J\,cm^{-2}}$ was irradiated at normal incidence to the surface of the alignment layer for the first exposure, and the irradiation of unpolarized UV of $1.2\,\mathrm{J\,cm^{-2}}$ at 45° to the surface of the alignment layer was applied as the second exposure. The measured pretilt angles of E7 on the PMDA-BDAF-ODA polyimide were dependent on the BDAF content in the polyimide alignment layer and higher than that on the PMDA-ODA polyimide alignment layer. The pretilt angles of the LC increased with the BDAF content and the LC alignment was homeotropic for the F43 polyimide alignment layers. It has in fact already been reported that polyimide based on fluorine-containing diamine causes

high pretilt angles [7, 8]. This was considered to be due to the higher content of fluorine atoms with a low surface energy in the polyimide alignment layer [9].

### 3.4. *Relationship between order parameter and pretilt angle of the liquid crystal*

Figure 5 shows the change in the order parameter of a dye in the LC with BDAF content in the polyimide alignment layer. The order parameter was measured on samples of the LC containing an added dye by measuring the absorbances of the dye parallel and perpendicular to the polarization using a polarized UV spectrometer. The order parameter steadily decreases with increasing BDAF content. It is thus seen that the LC ordering is weakened with increase in the pretilt angle. The decreasing interaction with the alignment layer with increase in pretilt angle can then be related to the decrease in the LC ordering on the alignment layer [10].
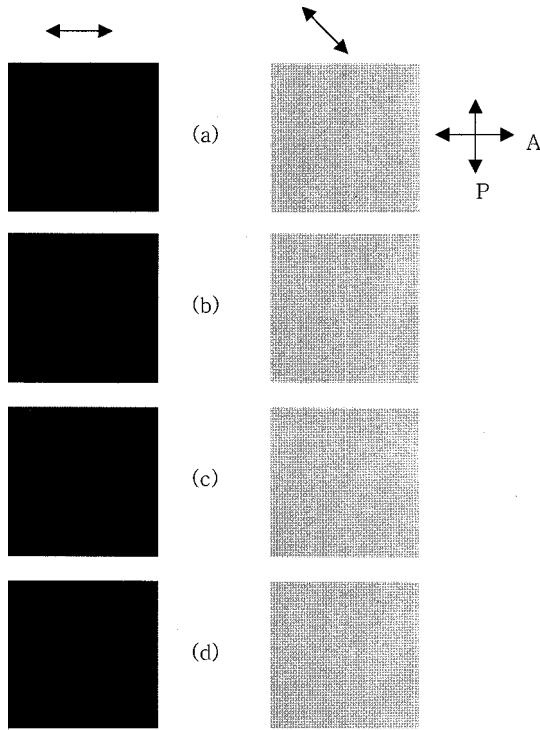
Figure 3. Polarized optical microscopic images for LC cells prepared with (*a*) F07, (*b*) F17, (*c*) F21, (*d*) F43.



Figure 4. Pretilt angle of E7 as a function of BDAF content in the polyimide alignment layer.

### 3.5. *Relationship between the surface energy of the alignment layer and the pretilt angle of the liquid crystal*

To investigate the reason for the increase in pretilt angle with BDAF content in the alignment layer, water and ethylene glycol contact angles were measured for varying BDAF content in the polyimide alignment layer. From these contact angle data, the surface energy of the alignment layer could be calculated using the following
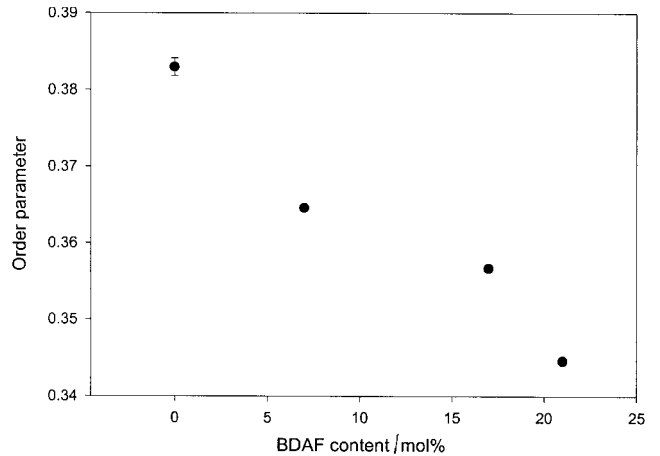


Figure 5. Order parameter of the LC as a function of the BDAF content in the alignment layer.

Girifalco–Good–Fowkers–Young equation:

$$1 + \cos \theta = 2 [ (\gamma_s^d \gamma_l^d)^{0.5} + (\gamma_s^p \gamma_l^p)^{0.5} ]/\gamma_l$$

$$\gamma^t = \gamma^d + \gamma^p.$$

Figure 6 represents the dependence of the surface energy on the BDAF content in the polyimide alignment layer. The total surface energy and the polar surface energy of the alignment layer are found to decrease with increasing BDAF content in the alignment layer, but the dispersion surface energy is shown to increase with BDAF content. Since the polar surface energy of the
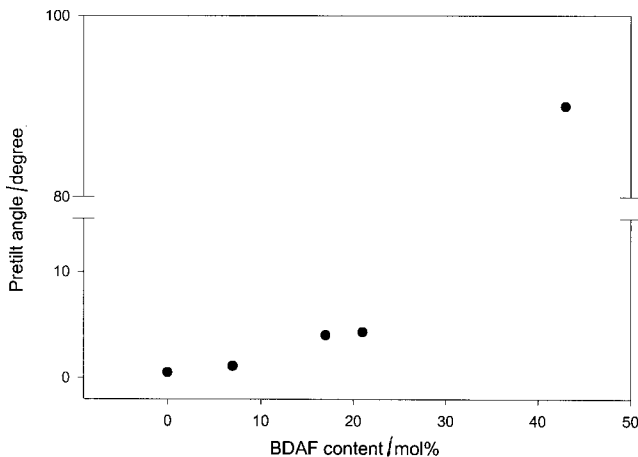


Figure 6. Surface energy of the alignment layer as a function of BDAF content of the copolymer.

alignment layer is most important for LC alignment, the pretilt angle is mainly affected by the polar surface energy [11]. As the polar surface energy of the alignment layer decreases, the interaction between LC and alignment layer becomes weaker and thus the pretilt angle increases.

### 3.6. *Surface morphology and chemical composition of the PMDA-BDAF-ODA polyimide alignment layer*

In order to elucidate the reason for the decrease in the polar surface energy with BDAF content in the polyimide alignment layer, the surface morphology and chemical composition of the polyimide alignment layer were investigated. These two factors are generally known to be responsible for LC alignment properties on alignment layers. The surface morphology of the polyimide alignment layer was observed by using a commercial atomic force microscope operated in a contact mode in air at room temperature. Figure 7 shows the morphology of the surfaces of a UV exposed alignment layer. The atomic force microscope images after the 60 min UV exposure showed us that the polarized UV exposure had induced changes in morphology of the surface of the polyimide alignment layer. The roughnesses of the non-exposed alignment layer and the 60 min UV-exposed alignment layer of F17 were found to be 0.183 and 0.305 nm, respectively. Considering the size of the LC molecules, such a small additional roughness of the polyimide alignment layer induced by the polarized UV exposure should have little influence on the surface energy of the alignment layer.

Spectroscopic analysis of the surface of the polyimide alignment layers was performed using XPS. Figure 8 shows the XPS spectra of the surfaces of F17 and F43 polyimide alignment layers exposed to polarized UV of 18 mW cm$^{-2}$. The peaks corresponding to the elements F, O, N and C are clearly observed. The relative surface atomic content of fluorine to that of carbon was 0.078 for F17 and 0.130 for F43. Due to the much higher fluorine atomic content of F43, the polar surface energy of F43 will be much lower. From the XPS analysis, it can be reasonably concluded that the amount of fluorine in the polyimide alignment layer is an important factor for pretilt angle generation.
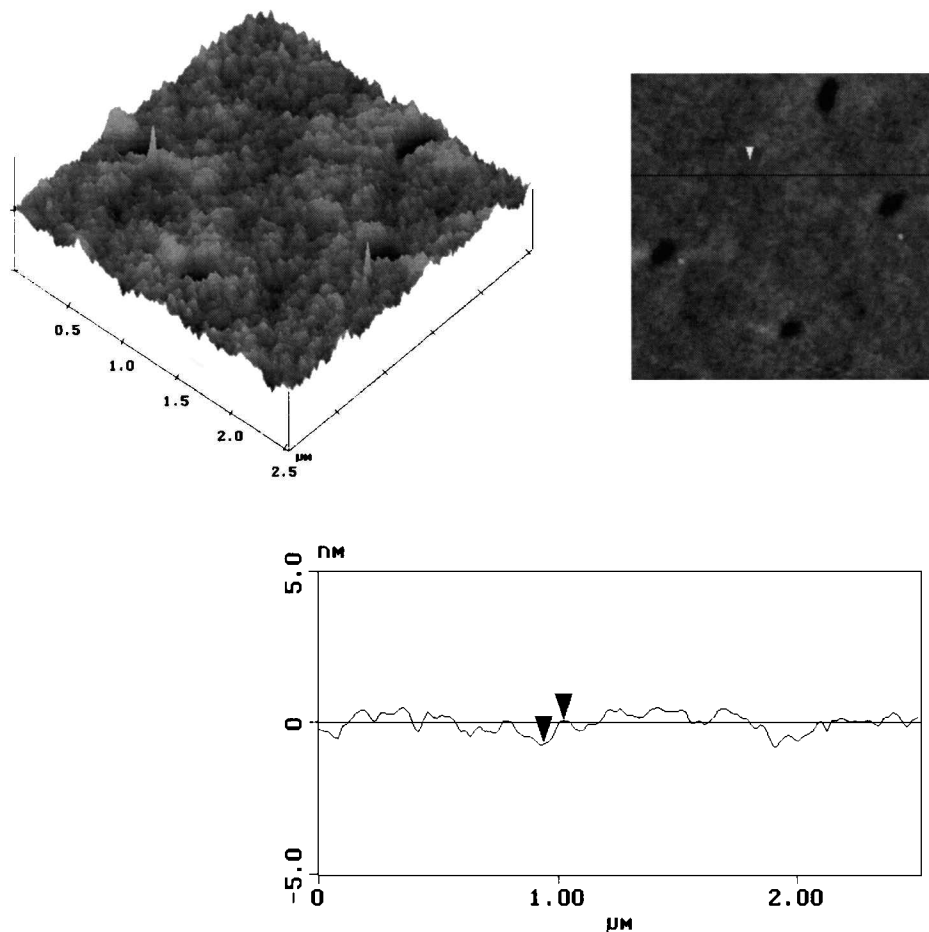


Figure 7. Surface analysis of the UV-irradiated F17 polyimide alignment layer.
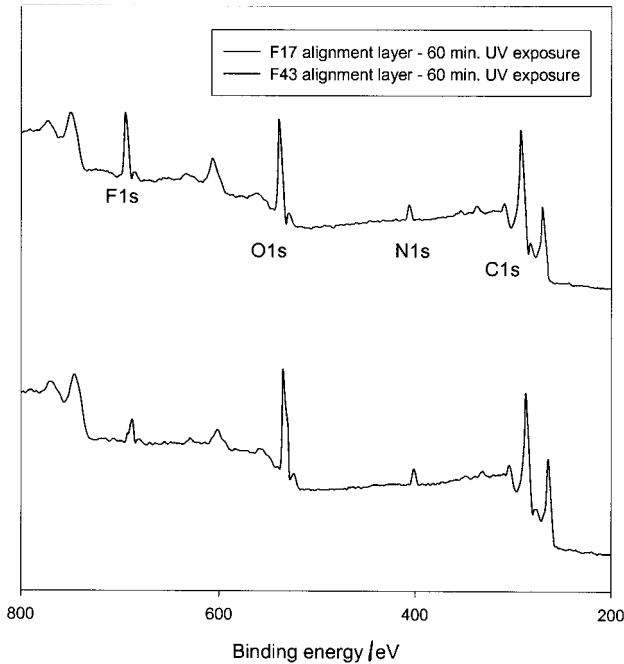
Figure 8. XPS spectra for (*a*) F17 and (*b*) F43 polyimide alignment layers.

### 3.7. *Relationship between UV exposure time and pretilt angle*

The pretilt angle of the LC on F07 and F17 alignment layers was investigated with varying UV exposure times. In our work, the modified double exposure method was used as described above. We irradiated with polarized UV for various times (10, 20, 40, 60 min) for the first exposure, and then with unpolarized UV for 1 min for the second exposure. Figure 9 shows the pretilt angle of the LC (E7) as a function of the first exposure time for the F07 and F17 alignment layers. By using the modified double exposure method, a pretilt angle greater than 1° could be generated for the polyimide alignment layers. With increasing UV exposure time, the pretilt angle of the LC is increased. For the F17 alignment layer, the pretilt angle of the LC was increased to 8° for the 60 min UV exposure. For the same UV exposure time, the pretilt angle of the F17 alignment layer was higher than that of the alignment layer based on F07 due to the higher fluorine content of the F17 alignment layer.

In order to investigate the reason for the increase in pretilt angle with polarized UV exposure time, the surface energy was measured as a function of varying UV exposure time using the method described earlier. Figure 10 represents the dependence of the surface energy of the polyimide alignment layer on the UV exposure time. Total and polar surface energies are found to decrease steadily with increasing UV exposure time. XPS analysis of the polyimide alignment layers was
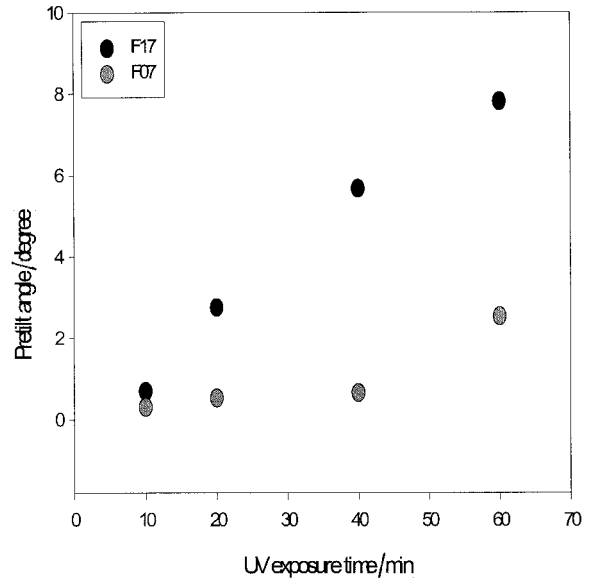


Figure 9. Plot of pretilt angle as a function of UV exposure time for F07 and F17 polyimide alignment layers.
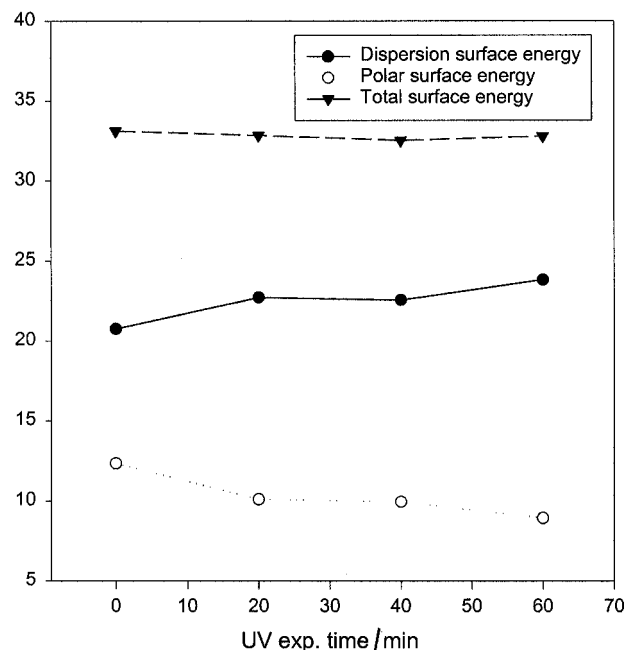


Figure 10. Surface energy of the alignment layer as a function of UV exposure time.

also performed with varying UV exposure time, and the surface atomic content relative to the carbon atom content was calculated (table 2). The UV-exposed alignment layer showed a higher fluorine atom content at the surface than for the unexposed alignment layer, resulting in a lower polar surface energy of the UV-exposed alignment layer. However, the effect of UV exposure time on the surface energy is less significant than the effect of the BDAF content of the alignment layer. From

Table 2. Relative surface atomic content of F17 samples measured from XPS analysis.

| Sample | C1s | O1s | N1s | F1s |
|---|---|---|---|---|
| Unexposed | 1 | 0.330 | 0.071 | 0.048 |
| 60 min UV-exposed | 1 | 0.361 | 0.074 | 0.078 |

these results, it can be reasonably concluded that the fluorine atom content in the alignment layer is an important factor for pretilt angle generation.

## 4. Conclusion

For PMDA-BDAF-ODA alignment layers, the pretilt angle gradually increases with BDAF content. The total surface energy and polar surface energy of the alignment layers decrease with BDAF content of the alignment layer and the dispersion surface energy increases with BDAF content. The pretilt angle also increases with UV exposure time. The polar surface energy decreases with UV exposure time, while the dispersion surface energy increases with UV exposure time. These results suggest that the increase in pretilt angle is related to the polar surface energy of the alignment layer. The change in surface morphology induced by UV exposure is so small that it seems to have little influence on the surface energy of the alignment layer.

## References

[1] LUO, F. C., 1990, *Liquid Crystals*, Vol. 1 (Singapore: World Scientific), p. 397.
[2] SEO, D. S., and KOBAYASHI, S., 1992, *Appl. Phys. Lett.*, **61,** 2392.
[3] BAN, B. S., and KIM, Y. B., 1999, *J. appl. polym. Sci.*, **74,** 267.
[4] OWENS, D. K., and WENDT, R. C., 1969, *J. appl. polym. Sci.*, **13,** 1741.
[5] SCHEFFER, T. J., and NEHRING, J., 1977, *J. appl. polym. Sci.*, **48,** 1783.
[6] IIMURA, Y., KOBAYASHI, S., HASHIMOTO, T., SUGIYAMA, T., and KATOH, K., 1990, *IEICE Trans. Elect.*, **E79-C,** 1040.
[7] FACTOR, B. J., RUSSEL, T. P., and TONEY, M. F., 1993, *Macromolecules*, **26,** 2847.
[8] CHEN, W., FELLER, M. B., and SHEN, Y. R., 1989, *Phys. Rev. Lett.*, **63,** 2665.
[9] IWAKABE, Y., HARA, M., KONDO, K., TOCHIGI, K., MUKOH, A., YAMADA, A., GARITO, A. F., and SASABE, H., 1991, *Jpn. J. appl. Phys.*, **30,** 2542.
[10] SUNG, S. J., LEE, J. W., KIM, H. T., and PARK, J. K., 2001, *Synth. Met.*, **117,** 277.
[11] BAN, B. S., and KIM, Y. B., 1999, *J. appl. polym. Sci.*, **74,** 267.